Changes in the thermal and structural properties of polylactide and its composites during a long-term degradation process

Jaroslav Cisar [1], Martina Pummerova [1,*], Petra Drohsler [1] and Vladimir Sedlarik [1,*]

[1] Centre of Polymer Systems, University Institute, Tomas Bata University in Zlín, Trida Tomase Bati 5678, 760 01 Zlín, Czech Republic; jcisar@utb.cz, pummerova@utb.cz, pvalkova@utb.cz, sedlarik@utb.cz

* Correspondence: pummerova@utb.cz; Tel.: +420 576 031 740 (MP); sedlarik@utb.cz; Tel.: +420 576 038 013 (VS)

Abstract: As a polymer degrades, its structure changes, the course of composting also affecting the rate and degree of decomposition. Moreover, the potential exists for the formation of microplastics. Since the process is complex, it was decided to investigate models reflecting the hydrolytic degradation of PLA-based composites at different temperatures (50, 55, and 60°C, respectively). Samples were prepared on semi-industrial equipment, thereby simulating actual production conditions. The effect of degradation temperature on their molecular weight was studied by gel permeation chromatography. Variation in the thermal properties and crystallinity of the PLA and its composites was investigated by differential scanning calorimetry and thermal gravimetric analysis. Mass loss during hydrolytic degradation was assessed using gravimetric technique, while confirmation of microplastic residues in the hydrolyzed samples was evaluated using Fourier-transform infrared spectroscopy.

Keywords: polylactide; polymer composite; calcium carbonate; plasticizer; hydrolysis; crystallinity

1. Introduction

Extensive research is being conducted to produce plastics from renewable sources, primarily in connection with polylactide (PLA). It offers several advantages, notably its favorable mechanical and optical properties, renewable origin and ability to decompose in the natural environment. However, the thermal and mechanical resistance of commercially available PLA, along with its barrier properties, are quite poor in comparison to conventional polymers [1-3]. As for practical applications, packaging and consumer goods, for example, require the use of thermostable PLA-based composites [4-6].

Adding a suitable filler is one approach to overcoming the inherent drawbacks of PLA [1]. However, challenges arise regarding the compatibility of the filler with PLA, which can result in phase separation and embrittlement in the resulting composites. Surface modification or the use of a plasticizer is typically required to improve filler dispersion and strengthen the interfacial bonding between the filler and the PLA matrix [7-9]. Employing low-molecular-weight plasticizers is a simple and cost-effective method to enhance the mechanical properties of PLA, extending its application in packaging area. The most commonly discussed plasticizers for PLA composites in the literature include citrate esters, poly(ethylene glycol) (PEG), glucose monoesters, glycerol, and oligomeric lactic acid, among others

[10,11]. The incorporation of PEG into PLA has been extensively studied, particularly due to its good biocompatibility and environmentally friendly attributes.

Studies [10-13] demonstrate that PEG-based additives have the ability to significantly plasticize PLA, increasing chain mobility and lowering the glass transition and cold crystallization temperatures. Plasticized PLA exhibits greatly enhanced ductility, with elongation at break increasing more than twentyfold compared to neat PLA. However, microphase separation often occurs in PEG-PLA blends, resulting in PEG migration to the surface of the film. Chemically modifying PEG chains is advantageous for improving plasticizing efficiency, as it helps to confine crystallization [10,12,14].

Calcium carbonate (CC) is a widely used, low-cost filler that enhances the modulus of elasticity, as well as heightening the strength, dimensional stability, gas permeability and physicochemical behaviour of PLA. Its presence in a composition, though, could affect the inherent biodegradability and disintegration profile of PLA-based materials [2,6,8,15,16]. It also affects the rate of hydrolysis [6], with studies reporting that CC possesses a high buffering capacity, maintaining a pH of approximately 7.4 and effectively neutralizing the acidic environment caused by PLA degradation [17,18].

Another critical aspect is the end-of-life of PLA-based composites once they become waste [2]. PLA is often marketed as compostable; studies have focused on the disposal of such materials in industrial and domestic composting facilities [19]. Some studies claim that PLA is completely compostable [20,21], while others suggest it degrades very slowly under suboptimal conditions [22-25]. The degradation rate of PLA-based materials depends on factors such as crystallinity, molecular weight and its distribution, morphology, the presence of plasticizers and fillers, water diffusion rate into the polymer, type of stereoisomerism and sample properties like surface roughness, thickness and porosity [5,26-29].

Reports state that PLA degrades in two steps, starting with hydrolysis into low-molecular-weight oligomers, followed by microbial degradation into carbon dioxide, water and humus. This process of hydrolysis is primarily influenced by external factors such as temperature, moisture and pH [5,23]. Hydrolytic degradation is a frequent occurrence, induced by soluble oligomers diffusing from the surface, which leads to increased chain mobility, plasticization, chain scission and, ultimately, rapid degradation of the material [8].

A review of the literature revealed that De Santis et al. [30] and Pantani et al. [44] researched the crystallization kinetics of PLA. Their aims were to clarify the mechanism of crystallization and determine the associated morphology in molten and glassy states. Neither study addresses degradation processes, however. As mentioned above, degradation rates can be controlled by blending PLA with additives, plasticizers and inorganic fillers. Although

various polylactide compositions have been extensively investigated with the aim of enhancing properties and degradation processes, these studies primarily involved low-doped composites (usually up to 5%) [16,28].

Despite the existence of numerous reports on strategies for improving PLA-based materials for various applications, especially for tissue engineering [18,26,29], scant attention has been paid to the long-term hydrolytic degradation processes of PLA or plasticized PLA composites supplemented with CC fillers. The research presented herein aims to address this issue. Description is given of a comprehensive, long-term investigation of morphological changes that occur in PLA during degradation under abiotic conditions at various temperatures, with a focus on the influence of inorganic fillers and amphiphilic block copolymers as plasticizers.

2. Materials and Methods

2.1. Materials

L-lactic acid 80% (LA; Lach-Ner, Neratovice, Czech Republic), polyethylene glycol (PEG; Mn ~8,000 g·mol^{-1}), the initiator Tin(II) 2-ethylhexanoate ($Sn(Oct)_2$, ~95%) (both from Sigma-Aldrich, Missouri, USA), methanol and acetone (p.a. grade; Penta, Prague, Czech Republic) were all utilized without further purification to synthesize the plasticizer (LA-PEG), as described below. As for the filler, industrial inorganic plate-shaped calcium carbonate (CC; food-grade; particle size 3.5 µm) was purchased from Fichema (Brno, Czech Republic). PLA Ingeo 2003D (NatureWorks, Minnesota, USA) was selected as the polymer matrix. A commercial grade material, comprising a D% comonomer of up to 4.25 ± 0.55% (melt flow index of 6; M_n = 145,000; M_w = 235,000), for which the glass transition (T_g) and melting point (T_m) temperatures equal 62 °C and 147 °C, respectively [30].

2.2. Plasticizer synthesis

The plasticizer (LA-PEG) was synthesized by direct melt polycondensation of LA and PEG in accordance with a procedure published in a study [12]. In brief, 500 ml of 80% LA solution was poured into a two-neck flask equipped with a Teflon stirrer and condenser. This was dehydrated at 160 °C under a reduced pressure of 20 kPa for 4 hours in an oil bath. The following step involved supplementation with 7.5 wt.% of PEG and 0.5 wt.% of $Sn(Oct)_2$, upon which the reaction continued under the reduced pressure of 3 kPa for 48 hours. The obtained product was then cooled down, dissolved in acetone, precipitated into a solution of distilled water/methanol at the ratio of 1:1, filtrated and washed with distilled water several times. The resultant product, a powder with an Mw of 6,000 g·mol$^{-1,}$ was dried at 50 °C for 24 hours.

2.3. Samples preparation procedure

A form of semi-crystalline polylactic acid (PLA Ingeo 2003D) was selected for the experiments, as it is specifically intended for the extrusion or thermoforming of packaging for fresh foodstuffs or food service ware. The PLA granules were dried in an oven under recommended conditions (60 °C, 12 hours). Fabrication followed of a composite comprising the PLA as the polymer matrix, the filler $CaCO_3$ (CC) and the polyester-based plasticizer (LA-PEG). This was carried out on a laboratory counter-rotating twin-screw extruder (LTE26, LabTech Engineering Company Ltd., Samut Prakan, Thailand) at a screw speed of 200 rpm and processing temperatures of 110-200°C. The resultant mixtures (Table 1) were cooled in a water bath, pelletized and dried at 60 °C for 4 hours for further

preparation. A single-screw extrusion unit was subsequently employed (LE45-30/CV, LabTech Engineering Company Ltd., Samut Prakan, Thailand), equipped with a flat extrusion head for producing films sized 250 mm wide and approximately 0.5 mm thick. The processing parameters were set as follows: chamber zone temperatures of 150 °C, 180 °C, 195 °C and 215 °C; the flat extrusion head at 205 °C; and a screw rotation of 20 rpm. The three cooling cylinders had temperatures of 60, 55 and 40 °C, respectively; these ran at the speed of 0.7 $m \cdot s^{-1}$ for gradual cooling, based on the setup of the extrusion unit. The formulations of the composite samples were informed by a study [12] and literature review [32-37], with adherence to the most widely applied concentrations of additives in the plastics industry. For comparison, a reference sample of the neat PLA matrix was prepared; the pre-dried granulate was directly extruded on a single-screw extrusion unit under identical conditions as described above.

Table 1. Sample compositions.

Name	**PLA content (wt.%)**	**$CaCO_3$ content (wt.%)**	**Plasticizer content (wt.%)**
PLA	100	-	-
PLA/CC	90	10	-
PLA/CC/LA-PEG	86	10	4

2.4. Methods

2.4.1. Sampling

The potential for defects in the processed samples was minimized by randomly removing pieces of neat PLA and composite foils for subsequent acceptance sampling; five distinct specimens were tested.

2.4.2. Gel permeation chromatography (GPC)

Analysis was conducted to discern alteration in the molar masses of the foils prior to and following the hydrolytic degradation process. The process began with dissolution in tetrahydrofuran (THF) stabilized with butylated hydroxytoluene (BHT), followed by filtration through a 0.45 µm syringe filter on a PL-GPC 220 chromatographic system (Agilent, Santa Clara, USA) equipped with dual detection device (a refractive index and viscometric detector). Separation was performed via 3 gel-mixed bed columns (Polymer Laboratories Ltd., Amherst, UK), a series comprising PLgel-Mixed-A bed column (300 × 7.8 mm, 20 µm), PLgel-Mixed-B bed column (300 × 7.8 mm, 10 µm) and PLgel-Mixed-D bed column (300 × 7.8 mm, 5 µm). The mobile phase contained the THF stabilized with BHT at 40 °C, the flow rate of the mobile phase was set to 1 $ml \cdot min^{-1}$ and the injection volume equalled 100 µl. The GPC system was calibrated with polystyrene standards for molecular weight over the range of 580–6,000,000 $g \cdot mol^{-1}$ (Polymer Laboratories Ltd., Amherst, UK). Results were expressed as the averages of three measurements.

2.4.3. Attenuated Total Reflection-Fourier-Transform Infrared (ATR-FTIR) Spectroscopy

The ATR-FTIR test is a suitable method for identifying the functional groups of polymers and the molecular structures of chemicals. In this study, it was used to identify characteristic peaks in the samples at the start of the test and to

compare them with the material residue (crystalline phase in powder form) after 5,000 hours of hydrolysis. ATR-FTIR spectra were obtained on a Nicolet iS5 instrument fitted with a diamond crystal (Thermo Fisher Scientific, Waltham, MA, USA). The resultant spectra in the wavenumber range from 400 to 4000 cm^{-1} represented averages of 64 scans at a spectral resolution of 0.8 cm^{-1}.

2.4.4. Thermogravimetric analysis (TGA)

Thermogravimetric analyses of samples in platinum crucibles were carried out on a TGA Series Q500 analyser (TA Instruments, Wilmington, USA). This occurred over the temperature range of 25 °C to 1000 °C, under a nitrogen atmosphere (60 ml·min^{-1}), at a heating rate of 10 °C·min^{-1}. The subsequent thermogravimetric (TGA) and derivative thermogravimetric curves (DTGA) expressed rates for weight loss as a function of temperature. Determination was made of the temperature at which 5% weight loss ($T_{5\%}$) occurred as well as the peak temperature (T_p) of the derivative of weight loss with respect to the DTGA temperature.

2.4.5. Differential scanning calorimetry (DSC)

The thermal properties of the materials were studied by DSC on a DSC1 STARe System (Mettler Toledo, Columbus, USA). Samples of ca 5 mg were placed in aluminium pans, hermetically sealed and inserted in the measuring cell. Measurements were taken under nitrogen (a flow rate of 50 ml·min^{-1}) in order to prevent oxidative degradation, at a heating/cooling rate of 10 °C·min^{-1}; the heating cycle started at 25 °C and rose to 180 °C, with subsequent cooling to 25 °C. The glass transition temperature (T_g) was determined from the resulting thermograms, defined as the midpoint of the heat capacity increment Temperatures for the peaks of the cold crystallization exotherm (T_{cc}) and melting endotherm (T_m), along with the enthalpies of physical transformation (ΔH_{cc} and ΔH_m, respectively) of the PLA matrix, were evaluated from the maxima and linear integration of peaks. Analysis was performed twice for each film sample with accurate results.

2.4.6. Abiotic degradation

Extruded foil samples of the PLA and composites were dried and weighed before being added into demineralized water in sterile screw flasks. Hydrolysis of samples took place at 50, 55, and 60 °C for 5,000 hours. In order to determine hydrolytic degradation, pieces of the polymeric and composite films were removed at predetermined intervals from the water medium, washed with fresh demineralized water and dried in a vacuum oven at 45 °C and 10 mbar to constant weight. These dried specimens were then weighed, and their weight loss in percent was calculated via the following equation:

$$\text{Weight loss (\%)} = [(W_0-W_1)/W_0]x100 \quad (1)$$

where W_0 is the initial weight of the sample and W_1 the dry weight of the sample after degradation.

2.4.7 Scanning electron microscopy

The morphology of the powder samples after hydrolytic degradation was analyzed using a Phenom Pro unit (Phenom-World BV, Eindhoven, The Netherlands) at an electron accelerating voltage of 5 kV.

3. Results and Discussion

The neat PLA foil and composites were characterized to discern their default parameters prior to undergoing hydrolytic degradation.

3.1. GPC

Findings for the molecular weights of the PLA, PLA/CC and PLA/CC/LA-PEG materials, respectively, are summarized in Table 2. No results were gauged for samples treated in water at different temperatures (50, 55, or 60 °C) since they possessed a crystalline structure. The methodology adopted herein encountered an issue regarding solubility connected with the cold crystallinity of PLA. At elevated temperatures and in an aqueous environment, the molecules in the amorphous regions of the PLA and composites had a tendency to rearrange into a more stable crystalline state. This transpired via an exothermic process, whereby the PLA was recrystallized during the hydrolytic degradation procedure. The phenomenon was continuously monitored by DSC analysis.

Table 2. GPC results for the nondegraded samples.

Name	M_n (g▾mol^{-1})	M_w (g▾mol^{-1})	M_p (g▾mol^{-1})	PDI (-)
PLA	103,000 ± 9,000	209,000 ± 5,000	215,000 ± 1,000	1.89 ± 0.37
PLA/CC	63,000 ± 5,000	128,000 ± 2,000	147,000 ± 4,000	2.05 ± 0.16
PLA/CC/LA-PEG	64,000 ± 4,000	122,000 ± 3,000	143,000 ± 3,000	1.91 ± 0.07

Table 2 shows that the neat PLA exhibited higher values for molecular weight values compared to both composites, due to the single thermal load applied during sample preparation. The composites originated from thermoplastically formed masterbatches, hence the thermal history of the materials was more pronounced. In other words, the shear stress and heating that transpired in the dual extrusion processes heightened the extent of thermo-mechanical degradation in the molecular weight distribution of the PLA composites [38]. This reduction in the molar weights of the composites, compared to the neat PLA foil, was anticipated and in agreement with the literature [39,40]. No significant difference was observed between the PLA/CC and PLA/CC/LA-PEG samples in this regard, indicating that the plasticizer in the composition had no substantial effect on molecular weight.

3.2. ATR-FTIR analysis

The utility of degradable materials such as PLA depends on their resistance to ageing processes. One of these is hydrolytic degradation by water, whereby water molecules diffuse into the polymer and hydrolysis of the matrix commences. Temperature and the pH of medium constitute crucial external factors in this context [5]. Figure 1 contains characteristic FTIR spectra for nondegraded samples of the amorphous neat PLA and composites, as well as for materials following 5,000 hours of degradation at 60 °C. The tested samples exhibit comparable spectral patterns in both graphs, typical of a PLA matrix. The spectral bands at 1045-1205 cm^{-1} and an absorption peak at 1755 cm^{-1} correspond to C—O and C═O stretching vibrations, respectively [41]. The C═O carbonyl stretching vibration is sensitive to morphology and conformation [41,42]. Absorption bands for the bending vibrations of C═O and OH functional groups are evident at 1225 cm^{-1} and 1050 cm^{-1}, respectively. The band at the lower wavenumber shows

some overlap, which complicates characterization [41,42]. The spectral band at 2850-3000 cm^{-1} is linked with a CH stretching vibration, consistent with the intrinsic molecular structure of PLA [41]. Figure 1 details the positions and shape of the bands pertaining to the structure and characteristics of the samples. Common to all the spectra are two bands relating to the crystalline and amorphous phases of PLA occurring in the regions of 755 cm^{-1} and 875 cm^{-1}. The first mentioned is assigned to the crystalline phase, while the latter relates to the amorphous phase, in good agreement with the findings of the DSC analysis [43,44]. All the degraded samples possess spectral bands at 680-880 cm^{-1} and 1350-1450 cm^{-1}, attributed to out-of-plane CH bending vibrations and C=C stretching vibrations, respectively. This suggests the formation of unsaturated hydrocarbon groups during hydrothermal degradation, likely caused by a transformation pathway involving the conversion of lactic acid (produced by the hydrolysis of PLA) into acetic acid via hydrothermal oxidation. This pathway undergoes aldol condensation and dehydration as acidic catalysis transpires, giving rise to unsaturated ketonic acid [41].

Figure 1. ATR-FTIR analyses of a) nondegraded samples and b) samples degraded for 5,000 h at 60 °C.

3.3. TGA

The influence of PLA degradation on thermal stability was analyzed using TGA. Figure 2 and Table 3 present findings for the PLA and composites in nondegraded form and after 5,000 hours of hydrolytic degradation at certain temperatures (50, 55, and 60 °C). The results of the thermogravimetric measurements were evaluated as follows: T_5 (°C) – 5% weight loss; T_{50} (°C) – 50% weight loss; T_{95} (°C) – 95% weight loss; $\Delta T_{5\text{-}95}$ (°C) – the temperature difference between 5% and 95% weight loss; and T_p (°C) – the maximum degradation temperature.

Aliphatic polyesters do not possess high thermal stability. Since PLA is such a material, it undergoes initial thermal decomposition at temperatures above 300 °C (Table 3). For neat PLA, the initial 5% weight loss (the onset of degradation) occurs at 302 °C. The decomposition temperature T_5 for PLA/CC was 297 °C, while its filler ($CaCO_3$) decomposed at 676 °C. PLA/CC/LA-PEG dropped temperature T_5 at 268 °C, the same filler breaking down at 674 °C (see Fig. 2, Tab. 3). It means that the presence of the CC filler leads to a decrease in the onset of degradation of the PLA composite material. An even more pronounced effect of this type was observed for the composite with the

plasticizer. Structural changes during hydrolysis (at 50, 55, and 60 °C) altered the nature of the degradation process, resulting in two-step degradation of the sample (see Fig. 2). At higher temperatures, the thermal stability of PLA decreased, and the temperature range $\Delta T_{5\text{-}95}$ (°C) becomes larger with increasing temperature.

Rocha et al. [15] investigated the thermal stability of PBAT/PLA-based samples with 10 and 20 wt.% of CC. They concluded that adding the filler reduced the thermal stability to values lower than those of the neat polymer blend, due to the catalytic effect of CC in the cleavage of ester bonds; this finding is in agreement with the data in Figures 2b and 2c, as well as in the literature [45,46].

Figure 2. TGA and dTGA curves for samples of a) PLA, b) PLA/CC and c) PLA/CC/LA-PEG in nondegraded form and after 5,000 h of hydrolytic degradation at 50, 55, and 60 °C.

Table 3. TGA analysis of samples in nondegraded form and after 5,000 h of hydrolytic degradation at 50, 55, and 60 °C.

	T_5 (°C)	T_{50} (°C)	T_{95} (°C)	$\Delta T_{5\text{-}95}$ (°C)	T_p (°C)
PLA					
Nondegraded	301.8	330.5	346.8	16.3	336.3
50 °C	221.1	276.9	357.6	80.7	266.3
55 °C	206.3	263.7	373.9	110.2	260.8
60 °C	183.8	239.7	598.9	359.2	246.7
PLA/CC					
Nondegraded	297.1	328.1	-	-	332.8

					676.4
50 °C	229.6	280.0	326.6	46.6	286.7
55 °C	207.9	260.6	360.7	100.1	256.0 395.6
60 °C	195.5	250.6	555.5	305.9	252.1 391.0
PLA/CC/LA-PEG					
Nondegraded	267.6	311.8	-	-	320.0 674.2
50 °C	200.1	251.3	344.4	93.1	253.7
55 °C	203.2	256.8	388.7	131.9	255.2
60 °C	216.4	266.8	402.6	135.8	276.0

3.4. DSC

The composition of materials and hydrolysis conditions affect the morphology of polymer structures in different ways. In this experiment, structural changes in the crystalline phases of the samples were analyzed in detail using DSC. Sample foils of neat amorphous PLA, as well as PLA/CC and PLA/CC/LA-PEG composites, were placed in individual glass bottles containing deionized water, according to their composition, and sealed with screw caps. These were then placed in laboratory ovens set to the desired temperature. The time for exposure amounted to 5,000 hours, with sampling happening at defined intervals to determine weight loss, followed by DSC. Three temperatures were selected for test of the given water environment, namely 50, 55, and 60 °C, thereby permitting the water molecules to freely migrate into the polymer matrix. According to Tsuji et al. [47], this would induce an autocatalytic reaction, leading to the accumulation of catalytic oligomers formed by such hydrolysis.

Figure 3 presents the DSC results from the first scan for the tested specimens (neat PLA, PLA/CC, and PLA/CC/LA-PEG), with detailed results in Tables S1, S2, and S3 (see Supplementary file). Exposure to water gradually disrupted the crystalline phase in each sample, as indicated by the broadening of endothermic melting peaks and a shift to lower melting temperatures in the graphs.

The glass transition in the amorphous phase is associated with enthalpic relaxation caused by secondary molecular relaxation [48,49]. The T_g values of all nondegraded specimens are in a temperature range above 55 °C. PLA exhibited a T_g of 62.4 °C, while PLA/CC had a slightly higher T_g of 64.5 °C because of the supplemented filler. The presence of the plasticizer in the PLA/CC/LA-PEG foil reduced its T_g to 60.1 °C. A report in the literature [9] on PLA/organomontmorillonite/poly(ethylene glycol) (PEG) nanocomposites, prepared by a melt intercalation technique, described reductions induced by the PEG in the glass transition and crystallization temperatures of PLA, in

accordance with the findings herein. They described that the PEG in the composition raised the upper limit for moisture absorption of the PLA and decreased the diffusivity of the tested nanocomposites.

The crystalline structures of polylactide-based materials vary in accordance with the conditions under which crystallization takes place. The formation of such a structure for PLA and PLA/CC occurs in the solid phase (cold crystallization) and is denoted α. When PLA/CC/LA-PEG crystallizes at a temperature below 120 °C, a slightly different form of it is observed, referred to as α′. Its chain conformation and crystal formations are similar to the α structure, but have a somewhat looser and less ordered structure [7-9]. Both α and α′ crystal structures coexist within the temperature range of 100 °C to 120 °C [8-12].

PLA and PLA/CC crystallize at 95 °C to 135 °C, while PLA/CC/LA-PEG crystallizes in a lower temperature range, namely at 90 °C to 130 °C (see the Table S2 in the Supplementary section). According to the literature, the crystallization region of PLA typically ranges from 85 °C to 150 °C upon heating [4,13], although the fastest crystallization rate occurs between 95°C and 115°C [14]. The latter range is also reported by other authors as constituting the isothermal rate of crystallization [15-18]. The optimum temperature is around 110 °C for isothermal crystallization from melt [19]. Vidović et al. [16] described materials including PLA (Ingeo 3251D) composites with CC, fabricated by melt mixing in a Brabender plasticorder at 190 °C and supplemented with the given filler at the concentrations of 0.1, 1 and 5 wt.%. They studied the influence of the filler on the thermal properties and crystallinity of the prepared compositions. Results showed that neat PLA prepared in this way exhibited crystallization, while the filler hindered this phenomenon in the composites and improved their thermal stability.

The melting point of PLA lies between 130 °C and 180 °C depending on the content of L-lactide and the crystalline phase formed during crystallization [4]. The melting peak of PLA is single or double depending on the given crystalline form, the thickness of lamellae and the spherulites present. In addition, a double melting peak can be observed, suggesting that crystallization likely occurred within a temperature range where both the α and α' crystalline forms developed. [20]. The neat PLA sample exhibits a single melting peak (T_m = 146.7 °C), as does PLA/CC (T_m = 147.2 °C). In contrast, PLA/CC/LA-PEG shows a double melting peak (T_{m1} = 144.8 °C and T_{m2} = 151.0 °C), as detailed in Table S3 of the Supplementary file.

Figure 3. DSC curves for PLA, PLA/CC and PLA/CC/LA-PEG upon exposure to 50, 55, and 60 °C.

3.5. Abiotic degradation - Degradation rate versus crystalline phase content

The composting process follows a sequential mechanism, beginning with hydrolysis, which reduces the molecular weight of PLA, followed by microbial assimilation [4]. The initial step is an autocatalytic process that generates carboxylic acids, with lactic acid acting as a catalyst for hydrolysis. These transformation pathways were confirmed by FTIR analysis. Under the influence of moisture, the ester bonds in the main polymer chain underwent hydrolysis, primarily resulting in a reduced samples weight and water-soluble products formation [28]. Therefore, the research focused on hydrolytic degradation at different temperatures, with particular emphasis on changes in crystallinity within the structure. Abiotic hydrolysis experiments were conducted to determine whether temperatures near Tg accelerate PLA hydrolysis and lead to the formation of microplastic residues.

The literature [50] confirms that hydrolysis can occur not only at high temperatures, but also at relatively mild temperatures around 60 °C and under the influence of increased humidity, e.g. at industrial composting facilities. Several parameters affect its course, including prevailing environmental conditions such as water activity, temperature, pH and time. Other associated aspects comprise the degree of crystallization, molar mass, sample size and geometry, stereocomplex formation, number of acidic end groups and hydrophobicity also play a crucial role.

In the presence of water, after a certain time, hydrolysis of the ester groups commenced in the amorphous region of the tested materials, marking the second phase of the process during such exposure. Soluble oligomers and monomers formed by hydrolysis leached into the water, leading to a decrease in molecular weight [5]. Once the oligomers became degraded enough to dissolve, the PLA polymer and its composites experienced mass loss, which was more pronounced at higher temperatures in the aqueous environment, as shown in Figure 4. A significant difference in weight loss was observed between the water temperatures; at 50 °C, it was less than at 55 °C and 60 °C.

At all the tested temperatures, the trends for decomposition were similar, with PLA/CC decomposing the slowest. The rate for weight loss of the PLA sample at 50 °C stabilized at 43.12 ± 0.17 wt.% after 4,000 hours. At 55 °C and 60 °C, the decomposition of PLA and PLA/CC/LA-PEG transpired in an identical manner. The literature reports that the hydrolytic degradation of PLA nanocomposites begins at the interface between the two phases formed by PLA and the appropriate filler. [5].

After a certain time, hydrolytic degradation gradually leads to a decrease in the weight of the PLA sample, due to the formation and diffusion of water-soluble oligomers and low-molecular-weight monomers (e.g., hydroxy acids). [50-52]. Values for the total weight loss of the neat PLA samples in the aqueous environment at 50, 55, and 60 °C equaled 42.4, 91.8 and 99.4 wt.%, respectively, as presented in Figure 4. For the sake of comparison, a manuscript describing how materials degraded in a composting environment was referred to, specifically nano-reinforced PLA films which contained montmorillonite modified with an ammonium quaternary salt, CC or silicon dioxide were tested [2]. It was found therein that the film samples disintegrated to a great extent, with just traces of indistinguishable residue remaining after 6-7 weeks under the given composting conditions. In contrast, it was discerned herein that, over a similar period of time, merely a weight loss of up to 45 % transpired at usual temperatures in compost, as detailed in Figure 4. Under real conditions, therefore, the films degraded into microplastic residues; in this context, the values for PLA/CC dropped to 19.5, 66.8 and 96.1 wt.%, respectively. This finding is in agreement with other studies [53], in which fillers with a hydrophilic character absorbed more water than the PLA matrix, thereby complicating hydrolytic degradation and biodegradation of the material. The weight loss of PLA/CC/LA-PEG reached 56.1, 88.0, and 99.4 wt.% at the set temperatures. These results confirm that hydrolytic degradation does not necessarily result in the complete decomposition of the material [27,50].

Figure 4. Weight loss and the crystallinity content of a) PLA, b) PLA/CC and c) PLA/CC/LA-PEG at different temperatures.

The hydrolytic degradation of PLA and associated sample weight loss have been well documented. The process occurs primarily within the bulk of the material, rather than on its surface. The cleavage of polymer chains during hydrolysis occurs preferentially in the amorphous regions, increasing the overall crystallinity of the polymer. Consequently, hydrolysis is significantly faster in these regions than in semi-crystalline ones [50]. Macromolecular polymer chains in crystalline regions are more resistant to hydrolysis, compared to those in amorphous regions, as water molecules have very limited access to the chains inside the rigid crystalline areas [54]. This increases the content of the crystalline phase in the sample. Once a certain degree of crystallinity is reached, a plateau appears, followed by a tendency for a decrease (Figure 4) [55,56]. Slow hydrolysis of the chains at the surface of the crystalline regions then gradually commences, leading to their degradation. By the end of the experiment, merely a powdery residue remained from the original film samples after they had been dried. The degree of crystallinity, calculated from the mean melting enthalpy value of each group, was enhanced by nucleation; a phenomenon caused by supplementing the PLA matrix with additives, in agreement with the literature [26].

Water diffusion into the polymer matrix, effectively acting as a plasticizer, in combination with temperature, triggered a rapid rise in the crystalline phase content in the neat PLA, PLA/CC and PLA/CC/LA-PEG samples at the beginning of the experiment, especially in the amorphous materials (see Figure 4). Water penetrates the amorphous phase, and at elevated temperatures (above T_g) in an aqueous environment, PLA polymer molecules and PLA in composite materials tend to rearrange into a more stable crystalline state—a process known as PLA recrystallization (see the DSC curves in Figure 3). Additionally, the initial crystallization rate of PLA and its composites increases with rising aqueous temperatures.

3.6 Scanning electron microscopy

SEM micrographs of the PLA samples after 5,000 hours of hydrolysis at 50 (a), 55 (b) and 60 °C (c) are shown in the Figure 5. It can be noticed that the fragmentation of the samples is more intensive with increase temperature of the experiment. It is related to abovementioned results indication significantly higher PLA degradation rate above its glass transition temperature.

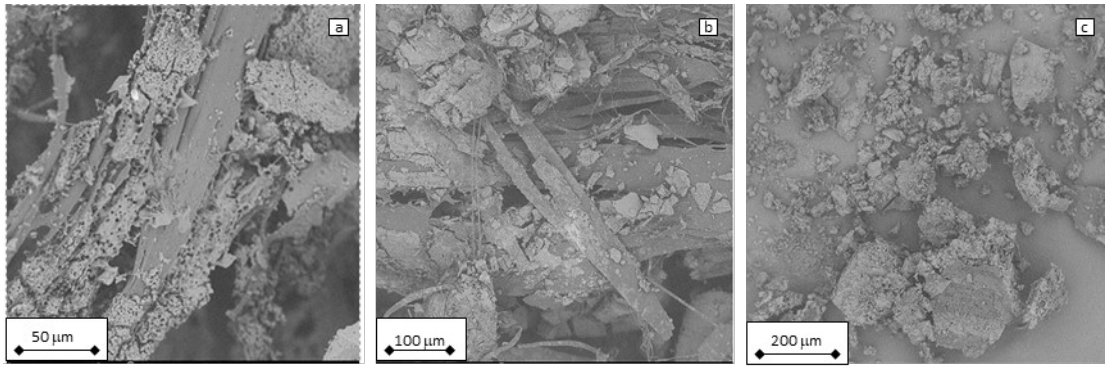

Figure 5: SEM micrographs of PLA sample after 5,000 hours hydrolysis at 50 (a), 55 (b) and 60 °C (c).

Fragments of the samples PLA/CC (a, b) and PLA/CC/LA-PEG (c, d) samples (5,000 hors, 60 °C) can be found in the Figure 6. The needle like residuals of CC is clearly visible there, while PLA fragments are not further visible.

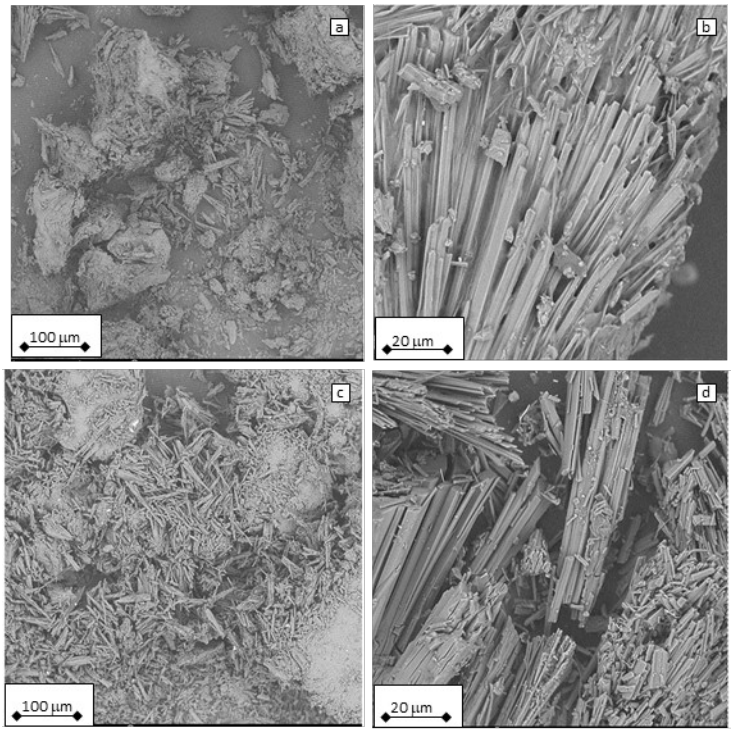

Figure 6: SEM micrographs of PLA/CC (a, b) and PLA/CC/LA-PEG (c, d) sample after 5,000 hours hydrolysis at 60 °C.

4. Conclusions

PLA and its composites belong among the most frequently used bioplastics-based materials. Despite broad research done on its degradation process, detailed analysis of its fate after longer time periods has not been reported. Findings reported in this work are important for evaluation of an environmental impact of the PLA and its composites after its lifetime but also after the time period defined by the standards for the biodegradation determination.

A detailed study was conducted on the morphological changes induced by the abiotic degradation of PLA, PLA/$CaCO_3$, and PLA/$CaCO_3$/LA-PEG systems at temperatures of 50, 55, and 60 °C over a period of 5,000 hours. The findings showed that the degradation process in the aqueous medium was significantly influenced by the morphology and volume fractions of the crystalline and amorphous regions. Hydrolytic degradation accelerated with increasing temperature (50 °C < 55 °C < 60 °C). Spectroscopy indicated the formation of unsaturated hydrocarbon groups, while DSC analysis revealed the gradual disruption of the crystalline phase, evidenced by the broadening of endothermic melting peaks and shifts in melting temperatures to lower values during hydrothermal degradation. As hydrolysis progressed, the foil samples fragmented into smaller particles. By the end of the experiment (5,000 hours), the dried particles measured less than 0.5 mm in size, so could be classified as microplastics.

Supplementary Materials: The following supporting information can be downloaded at: www.mdpi.com/xxx/s1, Figure S1: title; Table S1: title; Video S1: title.

Author Contributions: Conceptualization, J.C., M.P. and V.S.; methodology, J.C. and P.D.; validation, J.C.; formal analysis, J.C. and P.D.; investigation, J.C.; data curation, J.C. and M.P.; writing—original draft preparation, M.P.; writing—review and editing, M.P. and V.S.; visualization, M.P. and V.S.; supervision, V.S.; project administration, V.S.; funding acquisition, V.S. All authors have read and agreed to the published version of the manuscript.

Funding: This work was supported from the European Just Transition Fund within the Operational Programme: Just Transition under the aegis of the Ministry of the Environment of the Czech Republic, project CirkArena number CZ.10.03.01/00/22_003/0000045. Operational Programme Johannes Amos Comenius OP JAC "Application potential development in the field of polymer materials in the context of circular economy compliance (POCEK)", number CZ.02.01.01/00/23_021/0009004 and the development process of Centre of Polymer Systems, Tomas Bata University in Zlín, program DKRVO (RP/CPS/2024-28/002) were supported by the Ministry of Education Youth and Sports of the Czech Republic. Authors are further grateful for co-funding from the Technology Agency of the Czech Republic (project no. TQ03000235).

Institutional Review Board Statement: Not applicable.

Data Availability Statement: The original contributions presented in this study are included in the article. Further inquiries can be directed to the corresponding author.

Conflicts of Interest: The authors declare no conflicts of interest.

References

1. Kontou, E.; Niaounakis, M.; Panayiotis, G. Comparative study of PLA nanocomposites reinforced with clay and silica nanofillers and their mixtures. *J Appl. Polym. Sci.* **2011**, *122*, 1519-1529. DOI 10.1002/app.34234.
2. Balaguer, M.; Aliaga, C.; Fito, C.; Hortal, M. Compostability assessment of nano-reinforced poly(lactic acid) films. *Waste Manag.* **2016**, *48*, 143-155. DOI 10.1016/j.wasman.2015.10.030.
3. Gigante, V.; Coltelli, M.-B.; Vannozzi, A.; Panariello, L.; Fusco, A.; Trombi, L.; Lazzeri, A. Flat die extruded biocompatible poly(lactic acid) (PLA)/poly(butylene succinate) (PBS) based films. *Polymers* **2019**, *11*, 1857. DOI 10.3390/polym11111857.
4. Pantani, R.; Sorrentino, A. Influence of crystallinity on the biodegradation rate of injection-moulded poly(lactic acid) samples in controlled composting conditions. *Polym. Degrad. Stab.* **2013**, *51*, 1089-1096. DOI 10.1016/j.polymdegradstab.2013.01.005.
5. Olewnik-Kruszkowska, E. Influence of the type of buffer solution on thermal and structural properties of polylactide-based composites. *Polym. Degrad. Stab.* **2016**, *129*, 87-95. 10.1016/j.polymdegradstab.2016.04.009.
6. Shi, N.; Dou, Q. Non-isothermal cold crystallization kinetics of poly(lactic acid)/poly(butylene adipate-co-terephthalate)/treated calcium carbonate composites. *J. Therm. Anal. Calorim.*, **2015**, *119*, pp. 635–642. DOI 10.1007/s10973-014-4162-z.

7. Guo, H.; Zou, X.; Dai, W.; Zhang, P.; Xiao, B. Properties and morphology of polylactic acid composites reinforced by orientation aligned calcium carbonate whisker. *J Appl. Polym. Sci.* **2022**, *140*, e53622. DOI 10.1002/app.53622.

8. Chow, W. S.; Leu, Y. Y.; Mohd Ishak, Z. A. Water absorption of poly(lactic acid) nanocomposites: Effects of nanofillers and maleated rubbers. *Polym.-Plast. Technol. Mater.* **2014**, *53*, 858-863. DOI 10.1080/03602559.2014.886054.

9. Leu, Y. Y.; Chow, W. S. Kinetics of water absorption and thermal properties of poly(lactic acid)/organo montmorillonite/poly(ethylene glycol) nanocomposites. *J. Vinyl Addit. Technol.* **2011**, *17*, 40-47. DOI 10.1002/vnl.20259.

10. Turan, D.; Sirin, H.; Ozkoc, G. Effects of POSS particles on the mechanical, thermal, and morphological properties of PLA and plasticised PLA. *J Appl. Polym. Sci.* **2010**, *121*, 1067-1075. DOI 10.1002/app.33802

11. Zuo, U.; Chen, X.; Ding, Y.; Cui, L.; Fan, B.; Pan, L.; Zhang, K. Novel designed PEG-dicationic imidazolium-based ionic liquids as effective plasticizers for sustainable polylactide. *Chin. J. Chem.* **2021**, *39*, 2234-2240. DOI 10.1002/cjoc.202100217.

12. Cisar, J.; Drosler, P.; Pummerova, M.; Sedlarik, V.; Skoda, D. Composite based on PLA with improved shape stability under high-temperature conditions. *Polymer* **2023**, *276*, 125943. DOI 10.1016/j.polymer.2023.125943.

13. Li, Y.; Han, C.; Yu, Y.; Xiao, L.; Shao, Y. Crystallization behaviors of poly(lactic acid) composites fabricated using functionalized eggshell powder and poly(ethylene glycol). *Thermochim. Acta* **2018**, *663*, 67-76. DOI 10.1016/j.tca.2018.03.011.

14. Bhiogade, A.; Kannan, M.; Devanathan, S. Degradation kinetics study of Poly lactic acid (PLA) based biodegradable green composites. *Mater. Today* **2020**, *24*, 806–814. DOI 10.1016/j.matpr.2020.04.389.

15. Rocha, D. B.; Souza de Carvalho, J.; Aparecida de Oliveira, S. A new approach for flexible PBAT/PLA/$CaCO_3$ films into agriculture. *J Appl. Polym. Sci* **2018**, *135*, 46660. DOI 10.1002/app.46660.

16. Vidović, E.; Faraguna, F.; Jukić, A. Influence of inorganic fillers on PLA crystallinity and thermal properties. *J. Therm. Anal. Calorim.* **2017**, *127*, 371-380. DOI 10.1007/s10973-016-5750-x.

17. Gayer, C.; Ritter, J.; Bullemer, M.; Grom, S.; Jauer, L.; Meiners, W.; Schleifenbaum, J. H. Development of a solvent-free polylactide/calcium carbonate composite for selective laser sintering of bone tissue engineering scaffolds. *Mater. Sci. Eng. C* **2019**, *101*, 660-673. DOI 10.1016/j.msec.2019.03.101.

18. Donate, R.; Monzón, M.; Alemán-Domínguez, M. E.; Ortega, Z. Enzymatic degradation study of PLA-based composite scaffolds. *Rev. Adv. Mater. Sci.* **2020**, *59*, 170-175. DOI 10.1515/rams-2020-0005.

19. Polyák, P.; Nagy, K.; Vértessy, B.; Pukánszky, B. Self-regulating degradation technology for the biodegradation of poly(lactic acid). *Environ. Technol. Innov.* **2023**, *29*, 103000. DOI 10.1016/j.eti.2022.103000.

20. Kalita, N. K.; Damare, N. A.; Hazarika, D.; Bhagabati, P.; Kalamdhad, A.; Katiyar, V. Biodegradation and characterization study of compostable PLA bioplastic containing algae biomass as potential degradation accelerator. *Environ. Chall.* **2021**, *3*, 100067. DOI 10.1016/j.envc.2021.100067.

21. Ruggero, F.; Belardi, S.; Carretti, E.; Lotti, T.; Lubello, C.; Gori, R. Rigid and film bioplastics degradation under suboptimal composting conditions: A kinetic study. *Waste Manag. Res.* **2022**, *40*, 1311-1321. DOI 10.1177/0734242X211063.

22. Briassoulis, D.; Pikasi, A.; Hiskakis, M. Organic recycling of post-consumer /industrial bio-based plastics through industrial aerobic composting and anaerobic digestion - Techno-economic sustainability criteria and indicators. *Polym. Degrad. Stab.* **2021**, *190*, 109642. DOI 10.1016/j.polymdegradstab.2021.109642.

23. Hottle, T. A.; Agüero, M. L.; Bilec, M. M.; Landis, A. E. Alkaline amendment for the enhancement of compost degradation for polylactic acid biopolymer products. *Compost Sci. Util.* **2016**, *24*, 159-173. DOI 10.1080/1065657X.2015.1102664.

24. Kale, G.; Auras, R.; Singh, S. P.; Narayan, R. Biodegradability of polylactide bottles in real and simulated composting conditions. *Polym. Test.* **2007**, *26*, 1049-1061. DOI 10.1016/j.polymertesting.2007.07.006.

25. Guzman-Sielicka, A.; Janik, H.; Sielicki, P. Proposal of new starch-blends composition quickly degradable in marine environment. *J. Polym. Environ.* **2013**, *21*, 802-806. DOI 10.1007/s10924-012-0558-7.

26. Donate, R.; Monzón, M.; Alemán-Domínguez, M. E.; Rodríguez-Esparragón, F. Effects of ceramic additives and bioactive coatings on the degradation of polylactic acid-based bone scaffolds under hydrolytic conditions. *J. Biomed. Mater. Res. B* **2023**, *111*, 429-441. DOI 10.1002/jbm.b.35162.

27. Kucharczyk, P.; Hnatkova, E.; Dvorak, Z.; Sedlarik, V. Novel aspects of the degradation process of PLA based bulky samples under conditions of high partial pressure of water vapour. *Polym. Degrad. Stab.* **2013**, *98*, 150-157. DOI 10.1016/j.polymdegradstab.2012.10.016.

28. Liao, R.; Yang, B.; Yu, W.; Zhou, C. Isothermal cold crystallization kinetics of polylactide/nucleating agents. *J. Appl. Polym. Sci.* **2007**, *104*, 310-317. DOI 10.1002/app.25733.

29. Hoque, E. M.; Ghorban, D. M.; Khalid, M. Next generation biomimetic bone tissue engineering matrix from poly (L- lactic acid) PLA/calcium carbonate composites doped with silver nanoparticles. *Curr. Anal. Chem.* **2018**, *14*, 268-277. DOI 10.2174/1573411013666171003155024.

30. De Santis, F.; Pantani, R.; Titomanlio, G. Nucleation and crystallization kinetics of poly(lactic acid). *Thermochim. Acta* **2011**, *522*, 128-1334. DOI 10.1016/j.tca.2011.05.034.

31. Pantani, R.; De Santis, F.; Sorrentino, A.; De Maio, F.; Titomanlio G. Crystallization kinetics of virgin and processed poly(lactic acid). *Polym. Degrad. Stab.* **2010**, *95*, 1148-1159. DOI 10.1016/j.polymdegradstab.2010.04.018.

32. Andricic, B.; Kovacic, T.; Perinovac, S.; Grgic, A. Thermal properties of poly(L-lactide)/calcium carbonate nanocomposites. *Macromol. Symp.* **2008**, *263*, 96-101. DOI 10.1002/masy.200850312.

33. Aframehr, W. M.; Molki, B.; Heidarian, P.; Behzad, T.; Sadeghi, M.; Bagheri, R. Effect of calcium carbonate nanoparticles on barrier properties and biodegradability of polylactic acid. *Fibers Polym.* **2017**, *18*, 2041-2048. DOI 10.1007/s12221-017-6853-0.

34. Srihanam, P.; Thongsomboon, W.; Baimark, Y. Phase morphology, mechanical, and thermal properties of calcium carbonate-reinforced poly(L-lactide)-b-poly(ethylene glycol)-b-poly(L-lactide) bioplastics. *Polymers* **2023**, *15*, 301. DOI 10.3390/polym15020301.

35. Li, D.; Jiang, Y.; Lv, S.; Liu, X.; Gu, J.; Chen, Q.; Zhang, Y. Preparation of plasticized poly (lactic acid) and its influence on the properties of composite materials. *PLoS One* **2018**, *13*, e0193520. DOI 10.1371/journal.pone.0193520.

36. Nedaipour, F.; Bagheri, H.; Soheila, M. "Polylactic acid-polyethylene glycol-hydroxyapatite composite" an efficient composition for interference screws. *Nanocomposites* **2020**, *6*, 99-110. DOI 10.1080/20550324.2020.1794688.

37. Chaos, A.; Sangroniz, A.; Fernandez, J.; dol Rio, J.; Iriarte, M.; Sarasua, J. R.; Etxeberria, A. Plasticization of poly(lactide) with poly(ethylene glycol): Low weight plasticizer vs triblock copolymers. Effect on free volume and barrier properties. *J. Appl. Polym. Sci.* **2019**, *137*, 48868. DOI 10.1002/app.48868.

38. Muller, J.; Jimenez, A.; Gonzalez-Martinez, C.; Chiralt, A. Influence of plasticizers on thermal properties and crystallization behaviour of poly(lactic acid) films obtained by compression moulding. *Polym. Int.* **2016**, *65*, 970-978. DOI 10.1002/pi.5142.

39. Papadopoulou, K.; Klonos, P.A.; Kyritsis, A.; Tarani, E.; Chrissafis, K.; Masek, O.; Tsachouridis, K.; Anastasiou, A.D.; Bikiaris, D.N. Synthesis and characterization of PLA/biochar bio-composites containing different biochar types and content. Polymers **2025**, 17, 263. DOI 10.3390/polym17030263.

40. Backes, E. H.; Pires, L. D.; Costa, L. C.; Passador, F. R.; Pessan, L. A. Analysis of the degradation during melt processing of PLA/Biosilicate® composites. *J. Compos. Sci.* **2019**, *3*, 1-12. DOI 10.3390/jcs3020052.

41. Krishnudu, M. D.; Reddy, V. P.; Kumar, V. M.; Reddy, S. R.; Rao, U. A. Effect of $CaCO_3$ filler reinforcement on PLA matrix composites fabricated through injection moulding. *Phys. Scr.* **2024**, *99*, 065053. DOI 10.1088/1402-4896/ad4eae.

42. Yu, Y.; Zhu, B.; Ding, Y.; Zhou, C.; Ge, S. Impacts of poly(lactic acid) microplastics on organic compound leaching and heavy metal distribution during hydrothermal treatment of sludge. *Sci. Total Environ.* **2023**, *901*, 166012. DOI 10.1016/j.scitotenv.2023.166012.

43. Gbadeyan, O. L. Thermomechanical characterization of bioplastic films produced using a combination of polylactic acid and bionano calcium carbonate. *Sci. Rep.* **2022**, *15538*, 1-9. DOI 10.1038/s41598-022-20004-1.

44. Sun, Z.; Xu, S.; Zhang, B.; Zhong, J.; Dai, K.; Zheng, G.; Liu, C.; Shen, C. Supertoughened poly(lactic acid) containing low content of poly(ethylene oxide) with balanced mechanical property: The role of mesophase and phase morphology. *Polymer* **2024**, *295*, 126788. DOI 10.1016/j.polymer.2024.126788.

45. Nekhamanurak, B.; Patanathabutr, P.; Hongsriphan, N. The influence of micro-/nano-$CaCO_3$ on thermal stability and melt rheology behavior of poly(lactic acid). *Energy Procedia* **2014,** *56*, 118-128. DOI 10.1016/j.egypro.2014.07.139.

46. Kim, H.-S.; Park, B. H.; Choi, J. H.; Yoon, J.-S. Mechanical properties and thermal stability of poly(L-lactide)/calcium carbonate composites. *J. Appl. Polym. Sci.* **2008**, *109*, 3087-3092. DOI 10.1002/app.28229.

47. Tsuji, H.; Echizen, Y.; Saha, S. K.; Nishimura, Y. Photodegradation of poly(L-lactic acid): Effects of photosensitizer. *Macromol. Mater. Eng.* **2008**, *290*, 1192-1203. DOI 10.1002/mame.200500278.

48. Kalia, S.; Avérous, L. *Biodegradable and Biobased Polymers for Environmental and Biomedical Applications*, 1st ed.; Wiley: Hoboken, New Jersey, 2016; pp. 171-224. DOI 10.1002/9781119117360. 2016.

49. Dobircau, L.; Delpouve, N.; Herbinet, R.; Domenek, S.; Le Pluart, L.; Delbreilh, L.; Dacrue, V.; Dargent, E. Molecular mobility and physical ageing of plasticized poly(lactide). *Polym. Eng. Sci.* **2015**, *55*, 858-865. DOI 10.1002/pen.23952.

50. Dreier, J.; Brütting, C.; Ruckdäschel, H.; Altstädt, V.; Bonten, C. Investigation of the thermal and hydrolytic degradation of polylactide during autoclave foaming. *Polymers* **2021**, *16*, 2624. DOI 10.3390/polym13162624.

51. Odelius, K.; Hoglund, A.; Kumar, S.; Hakkarainen, M.; Ghosh, A. K.; Bhatnagar, N.; Albertsson, A.-C. Porosity and pore size regulate the degradation product profile of polylactide. *Biomacromolecules* **2011**, *12*, 1250-1258. DOI 10.1021/bm1015464.

52. Zhou, Z.; Zhou, J.; Yi, Q.; Liu, L.; Zhao, Y.; Nie, H.; Liu, X.; Zou, J.; Chen, L. Biological evaluation of poly-L-lactic acid composite containing bioactive glass. *Polym. Bull.* **2010**, *65*, 411-423. DOI 10.1007/s00289-010-0266-1.

53. Wolf, M. H.; Gil-Castel, O.; Cea, J.; Carrasco, J. C.; Ribes-Greus, A. Degradation of Plasticised Poly(lactide) Composites with nanofibrillated cellulose in different hydrothermal environments. *J. Polym. Environ.* **2023**, *31*, 2055-2072. DOI 10.1007/s10924-022-02711-y.

54. Gonzala, G. L.; Babetto, A. S.; Goncalves, L. M.; Bettini, S. H.; Souza, A. M. Biodegradation behavior of poly (lactic acid) samples obtained by three-dimensional printing: Influence of temperature and pigment presence. *Polym. Eng. Sci.* **2024**, *64*, 2812-2823. DOI 10.1002/pen.26727.

55. Kara, Y.; Molnar, K. Decomposition behavior of stereocomplex PLA melt-blown fine fiber mats in water and in compost. *J. Polym. Environ.* **2022**, *31*, 1398-1414. DOI 10.1007/s10924-022-02694-w.

56. Saadi, Z.; Rasmont, A.; Cesar, G.; Bewa, H.; Benguigui, L. Fungal degradation of poly(L-lactide) in soil and in compost. *J. Polym. Environ* **2012**, *20*, 273–282. DOI 10.1007/s10924-011-0399-9.